A COMPUTATIONALLY EFFICIENT METHOD FOR MULTISCALE MODELING OF COMPOSITE MATERIALS: EXTENDING MULTICONTINUUM THEORY TO COMPLEX 3D COMPOSITES

Ray S. Fertig, III
Firehole Technologies
210 South Third Street, Suite 202
Laramie, WY 82007

ABSTRACT

Accurate modeling of composite structures requires robust, computationally efficient multiscale modeling techniques. Multicontinuum theory (MCT), which allows constituent stresses and strains to be rapidly extracted from a composite strain state, is uniquely able to fill this need. Because MCT uses constituent-level stresses, simple failure criteria can be used to predict failure in structures comprised of complex composite microstructures. In addition, MCT has been readily integrated into finite element codes. The value of MCT for multiscale modeling of progressive failure in composite structures has already been demonstrated for unidirectional and woven composites, and elsewhere we have demonstrated its applicability physics-based fatigue life prediction in unidirectional composites. In this work MCT is generalized to any composite microstructure, using a recursive relationship between various groupings of composite constituent. Finally, an example is given of the utility of MCT in predicting failure in a braided composite.

1. INTRODUCTION

As microstructures of composite materials become more complex, such as in the case of three-dimensional woven architectures or multidirectional fabrics, accurate analysis of failure and progressive damage will become a limiting factor in ability of engineers to design with these materials. The challenge for the analyst is that failure in these materials is a complex event or series of events. For example, consider a triaxial braid microstructure, as shown in Figure 1. Failure can occur in any one of the three fiber tows or in the matrix materials surrounding the tows. Furthermore, different types of failure can occur within each tow: matrix cracking or fiber breakage. The consequences of each of these failures on the material response of the composite will be different. Thus, accurate design with these materials will require an analysis tool that can predict (a) which constituent of the composite will fail and (b) the effect of the constituent failure on composite response. Failures in these complex materials are unlikely to be accurately modeled by composite level quadratic failure criteria, such as Tsai-Wu. And the computational efficiency required by structural level finite element models precludes explicitly modeling all constituents during analysis. To achieve the required model fidelity to predict constituent failure while retaining the computational efficiency of simply applying failure criteria to the composite, we propose using multicontinuum theory (MCT) as the most viable method of failure prediction in complex composites.

MCT has been rigorously developed for both two-constituent [1],[2] and three-constituent composite materials [3],[4]. Essentially, MCT yields a closed-form solution that allows composite stresses and strains to be mapped to constituent stresses and strains. Using these *constituent stresses* we can apply relevant failure criteria, such as max stress or Tsai-Wu, at the *constituent level*. Thus, we can, without recourse to a micromechanics model, use the composite stress to predict which constituent will fail. For the purposes of modeling more complex composite microstructures, in this paper we develop the theory to extend to any *n*-constituent composite, regardless of the complexity of the composite. We demonstrate the accuracy of the MCT approach and then use it to predict an in-plane biaxial failure envelope for a triaxial braid microstructure similar to the one shown in Figure 1.

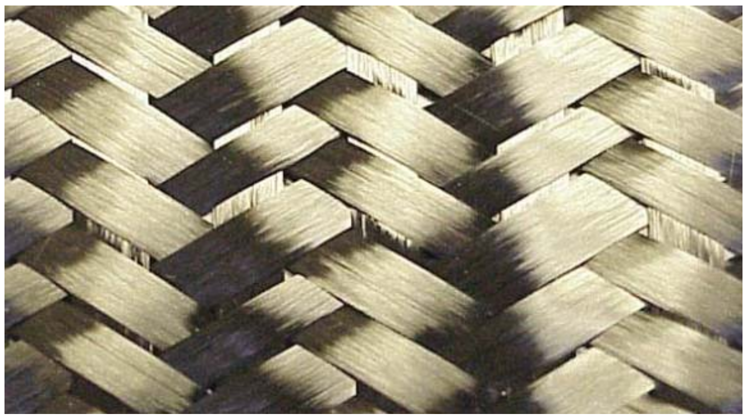

Figure 1. Triaxial carbon fiber braid with 60° yarns. (Reprinted with permission from S. P. Lomov, copyright (2010) by S. P. Lomov.)

2. MODEL DEVELOPMENT

2.1 Development of the n-constituent MCT decomposition

The defining feature of multicontinuum theory (MCT) is that it yields a closed-form linear relationship between composite strains and constituent stresses and strains. The constituent strain and stress, $\boldsymbol{\varepsilon}_i$ and $\boldsymbol{\sigma}_i$, respectively, can be written as

$$\begin{aligned} \boldsymbol{\varepsilon}_i &= \mathbf{Z}_i \boldsymbol{\varepsilon}_c + \boldsymbol{\Lambda}_i \Delta T \\ \boldsymbol{\sigma}_i &= \mathbf{Q}_i \boldsymbol{\varepsilon}_c + \boldsymbol{\Omega}_i \Delta T \end{aligned} \qquad [1]$$

where $\boldsymbol{\varepsilon}_c$ is the composite strain, $\mathbf{Z}_i$ is the transfer matrix relating composite strain to the volume average strain in constituent *i*, $\mathbf{Q}_i$ is the transfer matrix relating composite strain to the volume average stress in constituent *i*, $\boldsymbol{\Lambda}_i$ is a vector describing the temperature dependence of the strain of constituent *i*, $\boldsymbol{\Omega}_i$ is a vector describing the temperature dependence of the stress of constituent *i*, and ΔT represents the change in temperature from the stress free state. (In Section 2.1, repeated indices do not imply summation. Indices are use to delineate complete matrices and vectors.)

The relationship between constituent stress and strain and composite strains has already been rigorously developed elsewhere for two-constituent composites [1],[2]. This methodology has also been extended to three-constituent composites [3],[4]. Because the binary decomposition is the basis for the n-constituent decomposition derived in this paper, we briefly outline its development.

We assume linear elastic behavior of the composite and its constituents, such that the constitutive relationship is described by Hooke's Law.

$$\boldsymbol{\sigma}_i = \mathbf{C}_i \left(\boldsymbol{\varepsilon}_i - \boldsymbol{\eta}_i \Delta T \right) \qquad [2]$$

where $\mathbf{C}_i$ and $\boldsymbol{\eta}_i$ are the stiffness and thermal expansion vector, respectively, of material i (i = 1, 2, 12); material 12 is the composite comprised of constituents 1 and 2. Furthermore, the constituent averaged stresses and strains must sum to the composite stress and strain

$$\begin{aligned} \boldsymbol{\varepsilon}_{12} &= \psi_1 \boldsymbol{\varepsilon}_1 + \psi_2 \boldsymbol{\varepsilon}_2 \\ \boldsymbol{\sigma}_{12} &= \psi_1 \boldsymbol{\sigma}_1 + \psi_2 \boldsymbol{\sigma}_2 \end{aligned} \qquad [3]$$

where ψ_1 and ψ_2 are the volume fractions of constituents 1 and 2, respectively. Equations (2) and (3) can be used to solve for the transfer functions for constituent strains in the form described by Equation (1).

$$\begin{aligned} \mathbf{Z}_1 &= \frac{1}{\psi_1} \left(\mathbf{I} - \mathbf{Z}_2 \right) \\ \mathbf{Z}_2 &= \frac{1}{\psi_2} \left(\mathbf{I} - \left(\mathbf{C}_{12} - \mathbf{C}_1 \right)^{-1} \left(\mathbf{C}_{12} - \mathbf{C}_2 \right) \right)^{-1} \\ \boldsymbol{\Lambda}_1 &= \frac{1}{\psi_1} \left(\mathbf{C}_2 - \mathbf{C}_1 \right)^{-1} \left(\mathbf{C}_{12} \boldsymbol{\eta}_{12} - \psi_1 \mathbf{C}_1 \boldsymbol{\eta}_1 - \psi_2 \mathbf{C}_2 \boldsymbol{\eta}_2 \right) \\ \boldsymbol{\Lambda}_2 &= \frac{1}{\psi_2} \left(\mathbf{C}_2 - \mathbf{C}_1 \right)^{-1} \left(\mathbf{C}_{12} \boldsymbol{\eta}_{12} - \psi_1 \mathbf{C}_1 \boldsymbol{\eta}_1 - \psi_2 \mathbf{C}_2 \boldsymbol{\eta}_2 \right) \end{aligned} \qquad [4]$$

The transfer functions for stress can be obtained using Equation (2).

$$\begin{aligned} \mathbf{Q}_i &= \mathbf{C}_i \mathbf{Z}_i \\ \boldsymbol{\Omega}_i &= \mathbf{C}_i \left(\boldsymbol{\Lambda}_i - \boldsymbol{\eta}_i \right) \end{aligned} \qquad [5]$$

Extending this theory to composite materials with n-constituents requires treating the composite as a collection of super-constituents, each of which can be decomposed into a constituent and another super-constituent using a binary decomposition. Super-constituents are sub-level composites comprised of groups of constituents. The specific super-constituents may be chosen because of particular microstructural considerations or may be chosen arbitrarily. Decomposing the composite stress into n separate constituent stresses is accomplished by using $n-1$ successive binary decompositions. Except for the final decomposition, each decomposition results in the extraction of stresses and strains of one super-constituent and one constituent from the composite behavior. The final binary decomposition results in extracting stresses and strains of two constituents. This procedure is shown schematically in Figure 2 for a 5-constituent composite.

The development of the n-constituent MCT decomposition proceeds as follows. The goal of the MCT decomposition is to find $\mathbf{Z}_i$ and $\boldsymbol{\Lambda}_i$ (i = 1,2,…,n) as shown in Equation (1). Using n-1

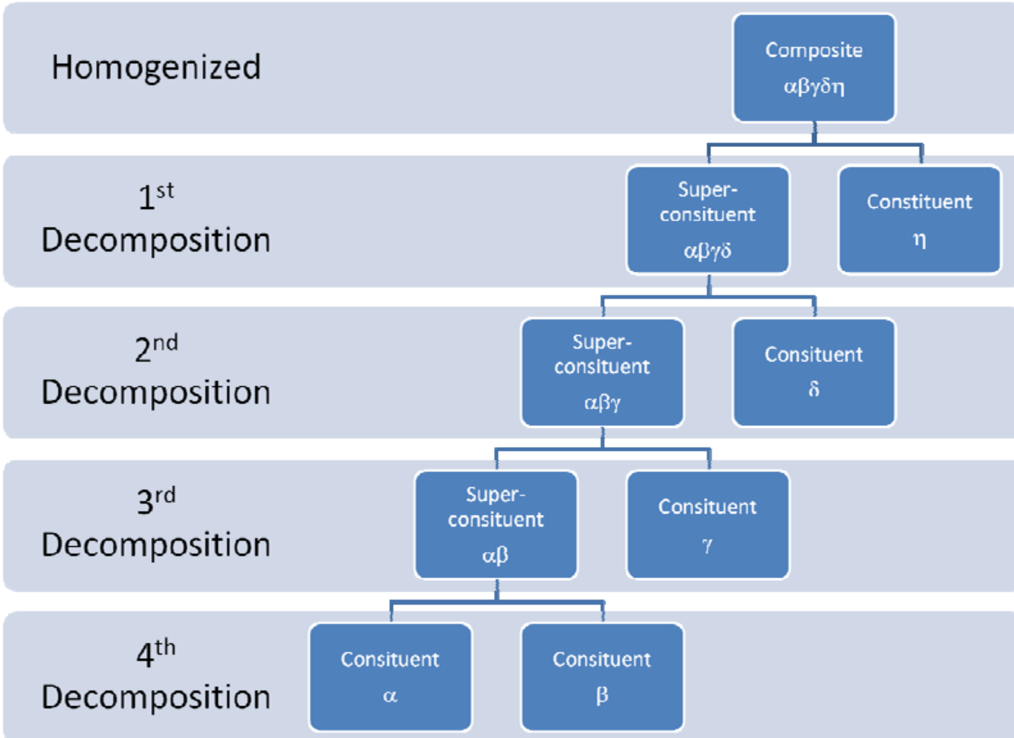

Figure 2. Tree of binary decompositions for a 5-constituent composite. The minimum number of decompositions required for n-constituents is n-1 decompositions.

binary decompositions, we obtain for each decomposition: (1) the transfer matrix $\mathbf{Z}_i'$ relating the strain of constituent i to the strain in the super-constituent obtained in the i-1 decomposition, (2) the transfer matrix ${}^i\mathbf{Z}_{sc}$ relating strain in the super-constituent of the i^{th} decomposition to the strain of the super-constituent in the i-1 decomposition, (3) the vector $\mathbf{\Lambda}_i'$ relating thermal strains in constituent i with the super-constituent in i-1, and (4) the vector ${}^i\mathbf{\Lambda}_{sc}$ relating thermal strains in super-constituent i with super-constituent i-1. Using Equation (4), these quantities can be calculated as

$$
\begin{aligned}
{}^i\mathbf{Z}_{sc} &= \frac{1}{{}^i\psi_{sc}}\left(\mathbf{I}-\mathbf{Z}_i'\right) \\
\mathbf{Z}_i' &= \frac{1}{\psi_i}\left(\mathbf{I}-\left({}^{i-1}\mathbf{C}_{sc}-{}^i\mathbf{C}_{sc}\right)^{-1}\left({}^{i-1}\mathbf{C}_{sc}-\mathbf{C}_i\right)\right)^{-1} \\
{}^i\mathbf{\Lambda}_{sc} &= \frac{1}{{}^i\psi_{sc}}\left(\mathbf{C}_i-{}^i\mathbf{C}_{sc}\right)^{-1}\left({}^{i-1}\mathbf{C}_{sc}\,{}^{i-1}\boldsymbol{\eta}_{sc}-{}^i\psi_{sc}\,{}^i\mathbf{C}_{sc}\,{}^i\boldsymbol{\eta}_{sc}-\psi_i\mathbf{C}_i\boldsymbol{\eta}_i\right) \\
\mathbf{\Lambda}_i' &= \frac{1}{\psi_i}\left(\mathbf{C}_i-{}^i\mathbf{C}_{sc}\right)^{-1}\left({}^{i-1}\mathbf{C}_{sc}\,{}^{i-1}\boldsymbol{\eta}_{sc}-{}^i\psi_{sc}\,{}^i\mathbf{C}_{sc}\,{}^i\boldsymbol{\eta}_{sc}-\psi_i\mathbf{C}_i\boldsymbol{\eta}_i\right)
\end{aligned}
\qquad [6]
$$

where $\mathbf{C}_i$ and ${}^i\mathbf{C}_{sc}$ are the stiffness matrices of constituent i and super-constituent of the i^{th} decomposition, respectively; ψ_i and ${}^i\psi_{sc}$ are the *relative* volume fractions of constituent i and the super constituent of the i^{th} decomposition, respectively; and $\boldsymbol{\eta}_i$ and ${}^i\boldsymbol{\eta}_{sc}$ are the coefficient of thermal expansion vectors of constituent i and super-constituent of the i^{th} decomposition, respectively.

The volume fractions in Equation (6) can be readily calculated from the volume fractions relative to the composite using

$$\psi_i = \frac{\phi_i}{\sum_{j=i}^{n} \phi_j}, \qquad {}^{i}\psi_{sc} = \frac{\sum_{j=i+1}^{n} \phi_j}{\sum_{j=i}^{n} \phi_j} \qquad [7]$$

where ϕ_i is the volume fraction of constituent i relative to the entire composite. The series of binary decompositions leads to recursive relationships describing the transfer functions in terms of the stiffnesses $\mathbf{C}_j$ of constituents $j \leq i$ and super-constituents ${}^{k}\mathbf{C}_{sc}$ for the k^{th} decomposition, where $k \leq (i-1)$.

$$\left.\begin{aligned} \mathbf{Z}_i &= \mathbf{Z}_i^{'}\left(\prod_{j=2}^{i} {}^{j-1}\mathbf{Z}_{sc}^{T}\right)^{T} \\ \mathbf{\Lambda}_i &= \mathbf{\Lambda}_i^{'} + \mathbf{Z}_i^{'}\left({}^{i-1}\mathbf{\Lambda}_{sc}\right) + \mathbf{Z}_i^{'}\sum_{j=1}^{i-2}\left[\left(\prod_{k=j+1}^{i-1} {}^{k}\mathbf{Z}_{sc}^{T}\right)^{T}\left({}^{j}\mathbf{\Lambda}_{sc}\right)\right] \end{aligned}\right\} \quad 1 < i < n \qquad [8]$$

In the case of $i = 1$, $\mathbf{Z}_1 = \mathbf{Z}_1'$ and $\mathbf{\Lambda}_1 = \mathbf{\Lambda}_1'$. In the case of $i = n$, $\mathbf{Z}_i' = {}^{i}\mathbf{Z}_{sc}$ and $\mathbf{\Lambda}_i' = {}^{i}\mathbf{\Lambda}_{sc}$. Substituting Equations (8) into Equations (5) yields the relationships to constituent stresses. With this methodology in place, we now turn to the problem of determining constituent and super-constituent stiffnesses and coefficients of thermal expansion.

2.2 Calculation of constituent elastic properties

As is obvious from Equation (6), in order to perform the necessary MCT decompositions the stiffnesses of the composite and all super-constituents and constituents must be calculated. The stiffnesses of the super-constituents and constituents must be in the same coordinate system as the composite stiffness. Moreover, these stiffnesses are *structural* stiffnesses. The structural stiffness is related to the composite-level contribution of a constituent to the composite stiffness—it may differ from the *material* stiffness at any given point in the constituent if the morphology of constituent varies throughout the composite representative volume element.

The stiffnesses of the composite and all super-constituents and constituents can be determined from six separate loadings of the composite. Super-constituent stresses and strains can be determined by summing the volume average stresses of the constituents comprising the super-constituent. Each loading condition k yields constituent volume-averaged stress and strain ${}^{k}\sigma_{ij}$ and ${}^{k}\varepsilon_{ij}$ for each constituent. (In Section 2.2, indices denote matrix or vector elements.) Assuming symmetry of the stiffness tensor, there are 21 elastic constants to be solved for, in the absence of material symmetry. When material symmetry is present, these equations can be simplified. Below we present the necessary equations required to solve for a constituent (or super-constituent) stiffness in the most general case, given six unique composite loadings.

$$\begin{bmatrix} {}^1\varepsilon_{11} & {}^1\varepsilon_{22} & {}^1\varepsilon_{33} & {}^1\gamma_{12} & {}^1\gamma_{13} & {}^1\gamma_{23} \\ \vdots & \vdots & \vdots & \vdots & \vdots & \vdots \\ {}^6\varepsilon_{11} & {}^6\varepsilon_{22} & {}^6\varepsilon_{33} & {}^6\gamma_{12} & {}^6\gamma_{13} & {}^6\gamma_{23} \end{bmatrix} \begin{Bmatrix} C_{11} \\ C_{12} \\ C_{13} \\ C_{14} \\ C_{15} \\ C_{16} \end{Bmatrix} = \begin{Bmatrix} {}^1\sigma_{11} \\ \vdots \\ {}^6\sigma_{11} \end{Bmatrix} \qquad [9]$$

$$\begin{bmatrix} {}^1\varepsilon_{22} & {}^1\varepsilon_{33} & {}^1\gamma_{12} & {}^1\gamma_{13} & {}^1\gamma_{23} \\ \vdots & \vdots & \vdots & \vdots & \vdots \\ {}^5\varepsilon_{22} & {}^5\varepsilon_{33} & {}^5\gamma_{12} & {}^5\gamma_{13} & {}^5\gamma_{23} \end{bmatrix} \begin{Bmatrix} C_{22} \\ C_{23} \\ C_{24} \\ C_{25} \\ C_{26} \end{Bmatrix} = \begin{Bmatrix} {}^1\sigma_{22} \\ \vdots \\ {}^5\sigma_{22} \end{Bmatrix} - C_{12} \begin{Bmatrix} {}^1\varepsilon_{11} \\ \vdots \\ {}^5\varepsilon_{11} \end{Bmatrix} \qquad [10]$$

$$\begin{bmatrix} {}^1\varepsilon_{33} & {}^1\gamma_{12} & {}^1\gamma_{13} & {}^1\gamma_{23} \\ \vdots & \vdots & \vdots & \vdots \\ {}^4\varepsilon_{33} & {}^4\gamma_{12} & {}^4\gamma_{13} & {}^4\gamma_{23} \end{bmatrix} \begin{Bmatrix} C_{33} \\ C_{34} \\ C_{35} \\ C_{36} \end{Bmatrix} = \begin{Bmatrix} {}^1\sigma_{33} \\ \vdots \\ {}^4\sigma_{33} \end{Bmatrix} - C_{13} \begin{Bmatrix} {}^1\varepsilon_{11} \\ \vdots \\ {}^4\varepsilon_{11} \end{Bmatrix} - C_{23} \begin{Bmatrix} {}^1\varepsilon_{22} \\ \vdots \\ {}^4\varepsilon_{22} \end{Bmatrix} \qquad [11]$$

$$\begin{bmatrix} {}^1\gamma_{12} & {}^1\gamma_{13} & {}^1\gamma_{23} \\ {}^2\gamma_{12} & {}^2\gamma_{13} & {}^2\gamma_{23} \\ {}^3\gamma_{12} & {}^3\gamma_{13} & {}^3\gamma_{23} \end{bmatrix} \begin{Bmatrix} C_{44} \\ C_{45} \\ C_{46} \end{Bmatrix} = \begin{Bmatrix} {}^1\sigma_{12} \\ {}^2\sigma_{12} \\ {}^3\sigma_{12} \end{Bmatrix} - C_{14} \begin{Bmatrix} {}^1\varepsilon_{11} \\ {}^2\varepsilon_{11} \\ {}^3\varepsilon_{11} \end{Bmatrix} - C_{24} \begin{Bmatrix} {}^1\varepsilon_{22} \\ {}^2\varepsilon_{22} \\ {}^3\varepsilon_{22} \end{Bmatrix} - C_{34} \begin{Bmatrix} {}^1\varepsilon_{33} \\ {}^2\varepsilon_{33} \\ {}^3\varepsilon_{33} \end{Bmatrix} \qquad [12]$$

$$\begin{bmatrix} {}^1\gamma_{13} & {}^1\gamma_{23} \\ {}^2\gamma_{13} & {}^2\gamma_{23} \end{bmatrix} \begin{Bmatrix} C_{55} \\ C_{56} \end{Bmatrix} = \begin{Bmatrix} {}^1\sigma_{13} \\ {}^2\sigma_{13} \end{Bmatrix} - C_{15} \begin{Bmatrix} {}^1\varepsilon_{11} \\ {}^2\varepsilon_{11} \end{Bmatrix} - C_{25} \begin{Bmatrix} {}^1\varepsilon_{22} \\ {}^2\varepsilon_{22} \end{Bmatrix} - C_{35} \begin{Bmatrix} {}^1\varepsilon_{33} \\ {}^2\varepsilon_{33} \end{Bmatrix} - C_{45} \begin{Bmatrix} {}^1\gamma_{12} \\ {}^2\gamma_{12} \end{Bmatrix} \qquad [13]$$

$$C_{66} = \frac{1}{{}^1\gamma_{23}} {}^1\sigma_{23} - C_{16}\,{}^1\varepsilon_{11} - C_{26}\,{}^1\varepsilon_{22} - C_{36}\,{}^1\varepsilon_{33} - C_{46}\,{}^1\gamma_{12} - C_{56}\,{}^1\gamma_{13} \qquad [14]$$

After using Equations (9)-(14) to determine the stiffnesses of the constituents, the coefficients of thermal expansion for any constituent or super-constituent can be determined from one thermal loading state in the composite. (The point-wise coefficients of thermal expansion must be already known.) This loading will yield a constituent volume-averaged thermal stress and strain vectors $\boldsymbol{\sigma}^{th}$ and $\boldsymbol{\varepsilon}^{\mathbf{t}h}$ for each constituent. The structural thermal expansion coefficient $\boldsymbol{\eta}$ can then be calculated using

$$\boldsymbol{\eta} = \frac{\mathbf{C}\boldsymbol{\varepsilon}^{th} - \boldsymbol{\sigma}^{th}}{\Delta T} \qquad [15]$$

2.3 Development of MCT influence coefficients

The methods described in Sections 2.1 and 2.2 are applicable to systems where a constituent stiffness can be defined and where there exists a meaningful coordinate system for the constituent. In complex composites, such as the triaxial braid, constituent stiffnesses may not exist. This is because the tows are curved and interact such that stress concentrates in different regions of the tow depending on the composite loading. (Technically speaking, plain weave composites also exhibit this problem, but the error introduced is minimal.) Nevertheless, the concept of a multicontinuum remains relevant. In the case where a constituent stiffness cannot be defined, we introduce MCT influence coefficients to address the problem.

As with the MCT decomposition described in Section 2.1, we assume linear elastic behavior. Thus, all load states can be superimposed. Using the six fundamental load cases for the composite, a mapping can be generated between composite stress (or strain) and constituent stress (or strain). This mapping is independent of varying material orientations through the microstructure. For example, the influence coefficients ${}_1\chi_i^a$ for constituent a under a pure σ_{11} composite load state are just

$$ {}_1\chi_i^a = \frac{\sigma_i^a}{\sigma_1^c} \qquad [16] $$

where i (i = 1, 2, .., 6) represents the six components of stress vector. Thus, for any composite load state, the stress i in constituent k is given by

$$ \sigma_i^a = \sum_{j=1}^{6} {}_j\chi_i^a \sigma_j^c \qquad [17] $$

The primary advantage of using MCT influence coefficients is that they can relate average composite stress to average stress in a constituent with *varying* material orientation. In the case of a complex fabric composite comprised of unidirectional tows, the tow stresses calculated are averaged along the fiber direction so that utilizing the MCT decomposition equations in Equations (8) produces average fiber and matrix stresses that are exact.

3. RESULTS

In this section we first present results to verify that the MCT approach described above produces results that are in agreement with finite element results. Following this validation, we examine failure in a triaxial braid lamina under a variety of biaxial load states in order to demonstrate the utility of using MCT for failure prediction in complex composites.

3.1 Model validation

To validate the *n*-constituent MCT approach described above, two different composite microstructures were considered: a unidirectional (two-constituent) and a triaxial braid (four-constituent). (The micromechanics model for the triaxial braid was created by Schultz [5].) These microstructures are shown in Figure 3 below. For this illustration, the IM7-8552 carbon-epoxy system was chosen. The properties of this system are shown in Table 1 for a fiber volume fraction of 0.7..

Table 1. Mechanical properties of the IM7/8552 carbon-epoxy system

	$E_{22} = E_{33}$ (GPa)	$E_{22} = E_{33}$ (GPa)	G_{12} (GPa)	$\nu_{12} = \nu_{13}$	ν_{23}
Fiber	242	18.96	12.20	0.28	0.28
Matrix	5.52	5.52	5.52	0.385	0.385
Fiber tows/unidirectional	170.0	13.19	6.03	0.310	0.415

Finite element micromechanics models were created for each of these microstructures. The unidirectional model was used compare the results from Equation (8) with the volume average constituent stresses. The triaxial braid model was used to compare the results of using MCT influence coefficients with the volume average constituent stresses. The volume average stresses predicted by the MCT approach were compared with the volume average stress predicted by the finite element model to demonstrate that the volume average stresses are accurately predicted by our method. Tables 2 and 3 show the comparison between finite element results and MCT predictions. In all cases, agreement with model stresses is exact.

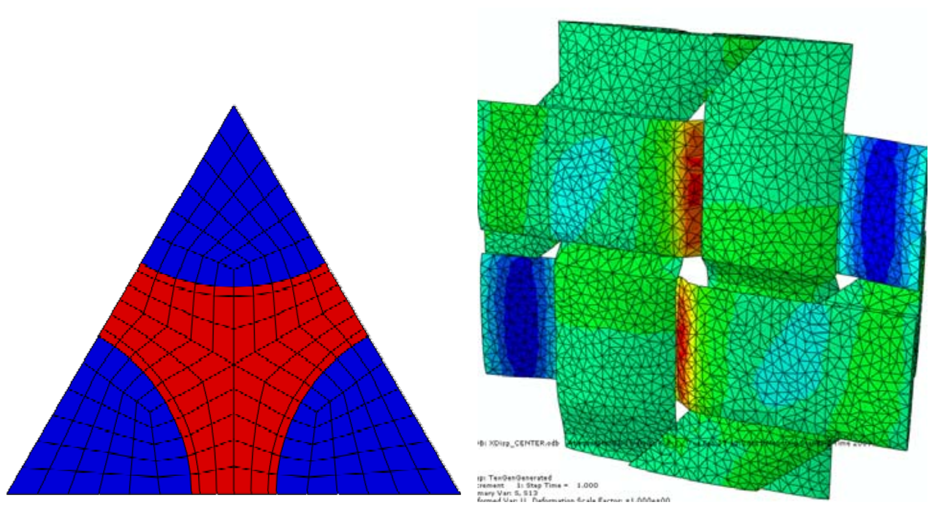

Figure 3. (Left) Representative volume element for a unidirectional microstructure. Blue indicates fiber; red indicates matrix. (Right) Triaxial braid microstructure. The matrix pocket surrounding the tows is not shown.

Table 2. Comparison of MCT decomposition (Equation (8)) with finite element results for unidirectional composite. All stresses are in units of MPa.

	σ_{11}	σ_{22}	σ_{33}	σ_{12}	σ_{13}	σ_{23}
Composite	50	30	10	15	15	15
Fiber						
FE	67.9	31.8	9.13	17.98	17.98	17.01
MCT	67.9	31.8	9.13	17.98	17.98	17.01

Matrix						
FE	18.62	26.8	15.52	9.75	9.75	11.47
MCT	18.62	26.8	15.52	9.75	9.75	11.47

Table 3. Comparison of MCT influence coefficient calculations with finite element results for a triaxial braid composite. All stresses are in units of MPa.

	σ_{11}	σ_{22}	σ_{33}	σ_{12}	σ_{13}	σ_{23}
Composite	5.342	6.678	-10.00	-4.007	3.536	3.536
Inlay tow						
FE	-4.25	-3.68	-13.34	-9.23	3.78	3.78
MCT	-4.25	-3.68	-13.34	-9.23	3.78	3.78
Cross tow1						
FE	50.9	3.03	-9.77	-5.58	4.44	3.76
MCT	50.9	3.03	-9.77	-5.58	4.44	3.76
Cross tow 2						
FE	2.52	59.35	-9.34	-5.56	3.76	4.45
MCT	2.52	59.35	-9.34	-5.56	3.76	4.45
Matrix pocket						
FE	-1.236	-0.954	-9.561	-2.44	3.27	3.27
MCT	-1.236	-0.954	-9.561	-2.44	3.27	3.27

3.2 Example: Predicted failure envelope of a triaxial braid composite

As a brief example of the utility of the MCT approach, we use it to predict a biaxial matrix failure envelope in the triaxial braid composite (Figure 3c). This was accomplished in four steps. First, influence coefficients are calculated for each tow in the triaxial braid and the transfer functions are calculated for the unidirectional composite—as described Section 2 above. Second, a failure criterion was chosen to apply to the matrix constituent inside each tow, and the failure coefficients were calibrated from unidirectional strengths. Third, tow stresses averaged along the fiber direction are calculated using MCT influence coefficients; these stresses are decomposed into fiber and matrix stresses in each tow. Finally, the matrix failure criterion is applied to the matrix in each tow to determine the first tow to have matrix failure.

We apply a failure criterion to the matrix that accounts for shear and tensile terms, and has been successfully used to predict failure in unidirectional composites [6]. (For this example, we assume that the matrix pocket does not play a significant role in predicting initial matrix failure.) Unlike in traditional composite analyses where composite level stresses are used, matrix stresses in the fiber tows are used in the failure criterion. The matrix failure criterion is as follows:

$$B_t\{I_t\}^2 + B_{s1}I_{s1} + B_{s2}I_{s2} = 1 \qquad [8]$$

where

$$I_t = \frac{\sigma_{22} + \sigma_{33} + \sqrt{(\sigma_{22} + \sigma_{33})^2 - 4(\sigma_{22}\sigma_{33} + \sigma_{23}^2)}}{2}$$
$$I_{s1} = \sigma_{12}^2 + \sigma_{13}^2 \qquad [9]$$
$$I_{s2} = \tfrac{1}{4}(\sigma_{22} - \sigma_{33})^2 + \sigma_{23}^2$$

and the {} denote Macaulay brackets such that the value is zero if the encompassed quantity is negative. The values of B_i are determined from three composite static failure tests: transverse tension, transverse compression, and in-plane shear, all of which involve failure of the matrix constituent.

The predicted failure envelope for in-plane loading of the triaxial braid composite is shown in Figure 4. The black curve outlines the failure envelope; the red squares indicate the region of the curve caused by matrix failure in cross tow 1; the blue circles indicate the region of the curve caused by matrix failure in cross tow 2; the green triangles indicate the region of the curve caused by matrix failure in the inlay tow. Using the MCT approach, these results only took less than a second to generate, after material characterization and show the ability of MCT to handle *any* loading for a complex composite. Moreover, the failure mode is clearly indicated because each constituent is evaluated individually for failure, which would permit appropriate material property degradation in a progressive failure analysis.

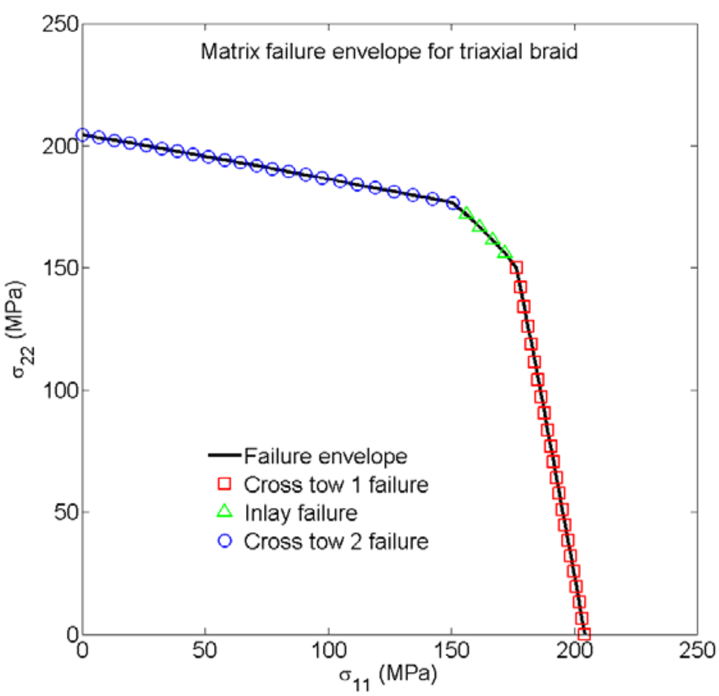

Figure 4. Failure envelope for the first quadrant with respect to in-plane normal stresses in principal material coordinates for the triaxial braid composite.

4. CONCLUSIONS

In this paper we have developed an *n*-constituent MCT approach, which relates composite stress (or strain) to constituent stress (or strain) using simple transfer functions derived from constituent stiffnesses. This method is applicable to any arbitrary composite microstructure and is extremely computationally efficient, since only a single matrix multiplication operation is required to extract constituent stresses. Knowledge of constituent stresses permits failure criteria to be applied at the constituent level, giving more accurate and higher fidelity failure predictions. Future work will involve fine tuning methods to determine in situ strengths of constituents from unidirectional composite or bulk material data.

5. ACKNOWLEDGEMENTS

This research was supported by the Air Force Office of Scientific Research (AFOSR) under contract number FA9550-10-C-0027 under the direction of Dr. David Stargel (Program Manager) and Dr. Edwin Forster (Technical Point of Contact).

6. REFERENCES

[1] M. Garnich and A. Hansen, "A Multicontinuum Theory for Thermal-Elastic Finite Element Analysis of Composite Materials," *Journal of Composite Materials*, vol. 31, Jan. 1997, pp. 71-86.

[2] M.R. Garnich and A.C. Hansen, "A Multicontinuum Approach to Structural Analysis of Linear Viscoelastic Composite Materials," *J Appl Mech*, vol. 64, Dec. 1997, pp. 795-803.

[3] C. Key, R. Six, and A. Hansen, "A three-constituent multicontinuum theory for woven fabric composite materials," *Composites Science and Technology*, vol. 63, 2003, pp. 1857-1864.

[4] R. S. Fertig, "An accurate and efficient method for constituent-based progressive failure modeling of a woven composite," *Supplemental Proceedings: Volume 2: Materials Characterization, Computation, Modeling and Energy*, Seattle, WA: TMS, 2010, pp. 223-230.

[5] J. Schultz, "Meso-scale and multicontinuum modeling of a triaxial braided textile composite," Master's thesis, University of Wyoming, 2009.

[6] R. S. Fertig, "Bridging the gap between physics and large-scale structural analysis: a novel method for fatigue life prediction of composites," *SAMPE*, 2009.